Spin-flip scattering in ZnTe—theoretical*

R. L. Hollis†
Department of Physics and Astrophysics, University of Colorado, Boulder, Colorado 80309
(Received 8 June 1976)

The valence-band energy levels of ZnTe in a magnetic field are computed using the Luttinger-Kohn formalism for zinc-blende semiconductors and experimental valence-band parameters obtained from cyclotron resonance. The results are used to obtain gyromagnetic ratios (g values) for light and heavy holes and applied to spin-flip scattering of laser light in the ZnTe valence band. The two shallowest-heavy-hole g values are found to be $g = 0.92 \pm 0.15$ and $g = 2.14 \pm 0.20$ in spherical approximation. The shallowest-light-hole value is found to be $g = 2.33 \pm 0.40$ in spherical approximation. Calculations are also presented for the magnetic field in the [111] crystallographic direction, and the magnetic field in the $(1\bar{1}0)$ plane. The effects of scattering from holes with finite momenta along the magnetic field are also considered. The g value of the shallowest-heavy-hole level is compatible with experiment.

I. INTRODUCTION

In recent years, optical studies of semiconductors in magnetic fields have yielded a wealth of information on band structure and defect complexes. Most of this work has focused on optical absorption and emission processes. A relatively new experimental technique, that of spin-flip scattering of laser light, is emerging as an important tool for such studies.

The principal information obtainable from a spin-flip scattering experiment is the gyromagnetic ratio or g value of the particles involved in the scattering process. In the case of electron spin-flip Raman scattering, the g values of free and bound electrons have been generally well-accounted for by theory. For hole spin-flip Raman scattering in the valence band of a semiconductor there have been no calculations of g values to date.

The purpose of this paper is to present calculations for the g values of heavy holes in ZnTe, motivated by the experimental results on ZnTe to be presented in a separate paper.[1] Fortunately, the theory of valence-band eigenfunctions and energy levels for zinc-blende semiconductors has already been developed by Luttinger and Kohn,[2,3] and will serve as the basis for the calculations which follow.

The existence of a nonzero cross section for spin-flip scattering from both holes and electrons was first demonstrated theoretically by Yafet in 1966.[4] An important feature of his work is the prediction that the cross section will diverge as the laser energy approaches the band-gap energy. Figure 1 provides an intuitive description of the spin-flip scattering process for holes in the valence band of a p-type semiconductor. In Fig. 1(a), the incident photon creates an electron-hole pair at t_1. At t_2 the electron combines with a spin-up hole, leaving a spin-down hole plus a photon. The intermediate state consists of two holes and an electron. The time-reversed process also contributes to the scattering cross section. Figure 1(b) shows the situation in a p-type semiconductor in a magnetic field. An incoming photon $h\nu$ excites an electron from below the Fermi level to a state near the conduction band. In Fig. 1(c), the electron returns to the valence-band level of op-

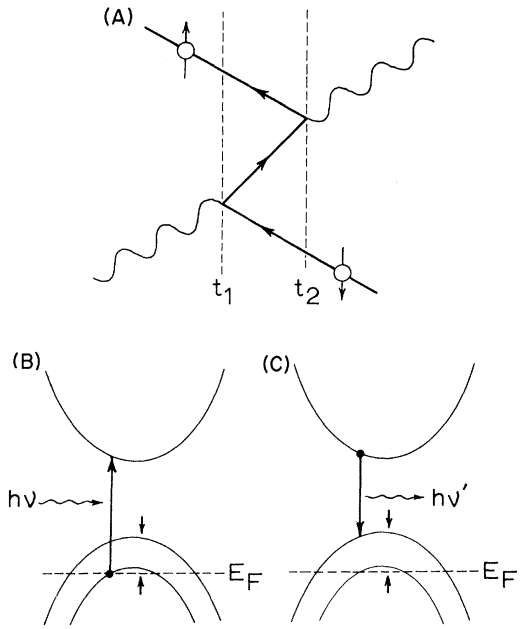

FIG. 1. Spin-flip scattering from holes in the valence band of a p-type semiconductor (schematic). (a) Time-ordered graph. An electron-hole pair is created at t_1. At t_2, the electron combines with a spin-up hole, leaving a spin-down hole. (b) Incoming photon excites an electron from the valence band to a state near the conduction band. (c) Electron drops back into the state of opposite spin, with the emission of a photon.

posite spin, with a photon of energy $h\nu'$ leaving the system. In this case the energy change of the photon is equal to the splitting in the valence band. Hole levels in the valence band of a zinc-blende structure semiconductor are fourfold degenerate in the absence of a field, and actually cannot be depicted by a simple pair of spin-split levels as shown in Fig. 1. More complicated considerations are necessary.

II. THEORY

In the absence of spin and spin-orbit interaction, the zinc-blende valence bands belong to the Γ_4 or Γ_5 representation of the cubic group. Inclusion of spin creates the additional representations Γ_6, Γ_7, and Γ_8. The (zero-spin) Γ_5 states transform[2] as x, y, and z under the tetrahedral point group. The resulting three-band edge functions X, Y, and Z, respectively, behave like functions of unity angular momentum and are formed from p-like functions of the individual ions.[5] The Γ_6 conduction-band state is formed from s-like states of the individual ions.

With the inclusion of spin and spin-orbit interaction the original threefold degenerate valence band (sixfold degenerate including spin) breaks up into a fourfold degenerate $J=\frac{3}{2}$ state and a twofold $J=\frac{1}{2}$ state. These states are labeled Γ_8 and Γ_7, respectively. The Γ_8 state is the one of higher energy. The valence-band wave functions which are diagonal in the $|J,m_J\rangle$ representation are[2]

$$\begin{aligned}
u^{(\alpha)}_{1,0} &= \left|\tfrac{3}{2},\tfrac{3}{2}\right\rangle = (1/\sqrt{2})\,|\,(X+iY)\uparrow\rangle\,,\\
u^{(\alpha)}_{2,0} &= \left|\tfrac{3}{2},\tfrac{1}{2}\right\rangle = (1/\sqrt{6})\,|\,(X+iY)\downarrow -2Z\uparrow\rangle\,,\\
u^{(\beta)}_{3,0} &= \left|\tfrac{3}{2},-\tfrac{1}{2}\right\rangle = (1/\sqrt{6})\,|\,(X-iY)\uparrow +2Z\downarrow\rangle\,,\\
u^{(\beta)}_{4,0} &= \left|\tfrac{3}{2},-\tfrac{3}{2}\right\rangle = -(1/\sqrt{2})\,|\,(X-iY)\downarrow\rangle\,,\\
u^{(\alpha)}_{5,0} &= \left|\tfrac{1}{2},\tfrac{1}{2}\right\rangle = (1/\sqrt{3})\,|\,(X+iY)\downarrow +Z\uparrow\rangle\,,\\
u^{(\beta)}_{6,0} &= \left|\tfrac{1}{2},-\tfrac{1}{2}\right\rangle = (1/\sqrt{3})\,|\,(X-iY)\uparrow -Z\downarrow\rangle\,,
\end{aligned} \tag{1}$$

where the spin-up $|\uparrow\rangle$ and spin-down $|\downarrow\rangle$ functions have been introduced. These are simply the eigenstates for a $J=\frac{3}{2}$ particle. The labels $u_{n,k}$ refer to eigenfunctions for band index n and momentum k.

The phases of X, Y, and Z are chosen in such a way as to satisfy the requirements of time-reversal symmetry. The Kramers' doublet states are

$$u^{(\alpha)}_{1,0} = \left|\tfrac{3}{2},\tfrac{3}{2}\right\rangle\,,\quad u^{(\beta)}_{4,0} = \left|\tfrac{3}{2},-\tfrac{3}{2}\right\rangle$$

for the heavy-hole states, and

$$u^{(\alpha)}_{2,0} = \left|\tfrac{3}{2},\tfrac{1}{2}\right\rangle\,,\quad u^{(\beta)}_{3,0} = \left|\tfrac{3}{2},-\tfrac{1}{2}\right\rangle$$

for the light-hole states. Here the spin functions α and β are subject to the condition

$$\alpha = T\beta\,, \tag{2}$$

where T is the Kramers' time-reversal operator.[6] The split-off band states $|\frac{1}{2},\frac{1}{2}\rangle$ and $|\frac{1}{2},-\frac{1}{2}\rangle$ also form a doublet. These states are evidently not readily accessible to a spin-flip scattering experiment and hence will not be considered further.

Through Eqs. (1) and (2), the initial and final states in a valence-band spin-flip scattering experiment have been given a rigorous meaning. Transitions between α and β states of the same hole band are observable only by the application of a magnetic field which serves to destroy the time-reversal symmetry of the states. In the presence of a magnetic field, the α and β states will have different energies.

Luttinger and Kohn[2] consider a degenerate Γ_8 energy band in an external homogeneous field H directed along the z axis. The Landau gauge

$$\vec{A} = (-Hy,\,0,\,0) \tag{3}$$

is chosen for the vector potential. In this gauge, the energy levels and eigenstates are given by solutions of the coupled equations[3] (in units where $\hbar = 1$),

$$\sum_{j'}\left[D^{\alpha\beta}_{jj'}\left(p_\alpha+\frac{e}{c}A_\alpha\right)\left(p_\beta+\frac{e}{c}A_\beta\right)\right]F_{j'}(\vec{r}) = EF_j(\vec{r})\,. \tag{4}$$

In Eq. (4), the repeated indices α and β are to be summed over x, y, and z. The summation over j' is over the number of degenerate states in the band. The p_α are the usual quantum-mechanical momentum operators, and the F_j are given by the Luttinger-Kohn wave functions

$$\psi = \sum_j F_j(r)\,u_{j,0}\,, \tag{5}$$

where the $u_{j,0}$ are the unperturbed $k=0$ basis states given by Eqs. (1).

By making the defintion

$$k_\alpha = p_\alpha + (e/c)A_\alpha\,, \tag{6}$$

the matrix $D_{jj'}$ can be generated, defined by its elements:

$$D_{jj'} = D^{\alpha\beta}_{jj'}\,k_\alpha k_\beta\,. \tag{7}$$

This "Hamiltonian" matrix is 4×4 in the case of the fourfold degenerate Γ_8 band, and is expressible in terms of a set of 4×4 angular momentum matrices satisfying the commutation rules

$$[J_x,J_y] = iJ_z,\quad \text{etc.}, \tag{8}$$

$$J_x^2+J_y^2+J_z^2 = \tfrac{3}{2}(\tfrac{3}{2}+1) = \tfrac{15}{4}\,. \tag{9}$$

These are, of course, the angular momentum matrices appropriate for a spin-$\frac{3}{2}$ particle. The remarkable similarity of this formalism to that

of the Dirac four-component theory of the electron has been pointed out in the literature.[7]

The matrix D derived by Luttinger is expressed as[3]

$$D=(1/m)[(\gamma_1+\tfrac{5}{2}\gamma_2)\tfrac{1}{2}k^2-\gamma_2(k_x^2J_x^2+k_y^2J_y^2+k_z^2J_z^2) - 2\gamma_3(\{k_xk_y\}\{J_xJ_y\}+\{k_yk_z\}\{J_yJ_z\} + \{k_zk_x\}\{J_zJ_x\})+(e/c)\kappa\vec{J}\cdot\vec{H} + (e/c)q(J_x^3H_x+J_y^3H_y+J_z^3H_z)]. \quad (10)$$

Here the symmetrized product is defined by the notation

$$\{k_xk_y\}=\tfrac{1}{2}(k_xk_y+k_yk_x), \quad \text{etc.} \quad (11)$$

In Eq. (10), the new dimensionless parameters γ_1, γ_2, γ_3, κ, and q have been introduced. These five constants depend upon the material properties, some of which are obtainable from experiment.

The parameters γ_1, γ_2, and γ_3 are related to the cyclotron resonance parameters A, B, and C as[8]

$$\gamma_1=-A, \quad (12)$$

$$\gamma_2=-\tfrac{1}{2}B, \quad (13)$$

$$\gamma_3=\tfrac{1}{2}(\tfrac{1}{3}C^2+B^2)^{1/2}. \quad (14)$$

The parameters κ and q are not directly obtainable from classical cyclotron resonance experiments.[9] Estimates of their magnitudes can be made, however. Under the assumption that bands of atomic f-like character are far from the valence band,[10]

$$\kappa\approx\tfrac{1}{3}(B-A-2)+\tfrac{1}{2}(\tfrac{1}{3}C^2+B^2)^{1/2}. \quad (15)$$

The parameter q is difficult to estimate, but is related to the spin-orbit parameter. For Ge, Kohn[11] has estimated q to be approximately 0.01. According to Yafet,[10] q will be "small" when the spin-orbit splitting of the valence band is small compared to the energy separation of this band from the other bands with which it is connected by the spin-orbit interaction. He concludes that this is indeed the case for all known semiconductors. In view of these considerations, q will be taken to be zero in the calculations which follow.

In 1968, Stradling[12] performed cyclotron resonance measurements on ZnTe. This was the first reported cyclotron resonance from holes in a II-VI compound. The p-ZnTe acceptor concentration in his samples was of the order of 7×10^{15} cm^{-3} and the maximum hole mobility was about 6500 cm^2/V sec at 35 °K. The studies were performed in the range of 45 to 65 °K at a frequency of 155 GHz and magnetic fields from 0 to 80 kG. From the measured anisotropy of the effective masses, Stradling was able to compute the following valence-band parameters:

$$A=-4.0\pm0.2, \quad (16)$$

$$|B|=2.3\pm0.4, \quad (17)$$

$$|C|=2.0\pm1.0. \quad (18)$$

The Luttinger parameters for ZnTe can now be computed from Eqs. (12)–(14) and Eq. (15), using the values in Eqs. (16)–(18):

$$\gamma_1=4.00, \quad (19)$$

$$\gamma_2=1.15, \quad (20)$$

$$\gamma_3=1.29, \quad (21)$$

$$\kappa\approx0.054, \quad (22)$$

$$q\approx0. \quad (23)$$

III. ENERGY LEVELS

It has not been proven possible to obtain a general solution to Eq. (4) with the matrix D of Eq. (10). Instead, Luttinger was able to obtain solutions for three specific cases. All three cases are limited to the condition in which there is zero momentum along the direction of the magnetic field ($k_H=0$). In the first case, the Hamiltonian D is solved rigorously for a magnetic field which lies in the [111] crystallographic direction. In the second case, a solution is obtained for the case of spherical energy bands. In the third case, an approximate solution is obtained for a magnetic field lying anywhere within the $(1\bar{1}0)$ plane. Luttinger used specific 4×4 representations for the matrices J.

A. Case 1: magnetic field in [111] direction

The Schrödinger equation $D\psi=E\psi$ can be solved with the Luttinger ansatz[3]

$$\psi=\begin{bmatrix} c_1\phi_n \\ c_2\phi_{n+2} \\ c_3\phi_{n-2} \\ c_4\phi_n \end{bmatrix}, \quad (24)$$

where the ϕ_n are harmonic oscillator eigenfunctions. Equation (24) is valid for $n\geq2$. The resulting numerical matrix D is given by

$$D=\begin{bmatrix} e_1 & e_2 & e_3 & e_4 \\ e_2 & e_5 & 0 & e_6 \\ e_3 & 0 & e_7 & e_8 \\ e_4 & e_6 & e_8 & e_9 \end{bmatrix}, \quad (25)$$

where

$$e_1 = (\gamma_1 + \gamma_3)(n + \tfrac{1}{2}) + \tfrac{3}{2}\kappa + \tfrac{23}{8}q, \quad (26)$$

$$e_2 = -(2\gamma_3 + \gamma_2)[\tfrac{1}{3}(n+1)(n+2)]^{1/2}, \quad (27)$$

$$e_3 = -(\gamma_3 - \gamma_2)[\tfrac{2}{3}n(n-1)]^{1/2}, \quad (28)$$

$$e_4 = -q/\sqrt{2}, \quad (29)$$

$$e_5 = (\gamma_1 - \gamma_3)(n + \tfrac{5}{2}) - \tfrac{1}{2}\kappa - \tfrac{13}{8}q, \quad (30)$$

$$e_6 = (\gamma_3 - \gamma_2)[\tfrac{2}{3}(n+1)(n+2)]^{1/2}, \quad (31)$$

$$e_7 = (\gamma_1 - \gamma_3)(n - \tfrac{3}{2}) + \tfrac{1}{2}\kappa + \tfrac{13}{8}q, \quad (32)$$

$$e_8 = -(2\gamma_3 + \gamma_2)[\tfrac{1}{3}n(n-1)]^{1/2}, \quad (33)$$

$$e_9 = (\gamma_1 + \gamma_3)(n + \tfrac{1}{2}) - \tfrac{3}{2}\kappa - \tfrac{23}{8}q. \quad (34)$$

Eigenvalues and eigenfunctions of D can be computed numerically from Eqs. (25)–(34) to desired degrees of accuracy. For $n = 0, 1$, further solutions are obtained by choosing $c_3 = 0$ and solving the resultant 3×3 problem. Two additional meaningful solutions are obtained for $n = -1, -2$, by setting $c_1 = c_3 = c_4 = 0$.

Using the parameters γ_1, γ_2, γ_3, κ, and $q = 0$ obtained in Sec. III, the energy levels for the ZnTe valence bands with the magnetic field in the [111] direction can be computed by solving the secular equation resulting from Eq. (25). The energy levels, expressed in cm^{-1}, are given in Table I for $H = 100$ kG. Here, the states are labeled using the notation of Eqs. (35) and (36), to be given later. The energies are relative to the degenerate zero-point energy in the [111] direction in the absence of the magnetic field. The shallowest states are those of the heavy-hole ladder $\epsilon_{\bar{\beta}}$. The $k_H = 0$ ordering of the α and β states is reversed for light holes and heavy holes.

TABLE I. ZnTe energy levels in the [111] crystallographic direction $H = 100$ kG.

n	ϵ^{+}_{α}	ϵ^{+}_{β}	ϵ^{-}_{α}	ϵ^{-}_{β}
0	12.41	23.93	...	...
1	37.73	73.27	...	...
2	78.32	129.53	10.15	5.99
3	131.25	188.11	31.89	22.07
4	188.69	247.61	49.11	37.24
5	247.72	307.56	64.75	51.96
6	307.42	367.74	79.71	66.44
7	367.48	428.08	94.32	80.77
8	427.73	488.51	108.73	95.00
9	488.10	549.00	123.02	109.17
10	548.56	609.54	137.23	123.30
11	609.08	670.12	151.38	137.38
12	669.63	730.72	165.49	151.45
	light holes		heavy holes	

(Energies are in cm^{-1} at $k_H = 0$)

As the quantum number n increases, the spectrum approaches a set of uniformly spaced harmonic oscillator levels, corresponding to two cyclotron effective masses and two effective spin states. Note that for large n, the difference in energy between α and β spin states of a given hole ladder approaches the cyclotron resonance energy ω_c for that ladder. This is the "classical" regime studied in Stradling's cyclotron resonance experiments. The calculations presented in Table I are "exact" insofar as the effective mass approximation is valid for this system.

B. Case 2: spherical approximation

The special case $\gamma_2 = \gamma_3$ corresponds to the case of spherical energy surfaces. If the parameter q is also set equal to zero, the characteristic values of Eq. (4) can be obtained without resorting to numerical calculations. The question of whether these approximations are valid for actual physical systems in general and for ZnTe in particular will be the subject of later discussion.

With $\gamma_2 = \gamma_3 = \bar{\gamma}$ and $q = 0$, Eq. (25) consists of two 2×2 submatrices which are directly diagonalized[3] to yield

$$\epsilon^{\pm}_{\alpha}(n) = \gamma_1 n - (\tfrac{1}{2}\gamma_1 + \bar{\gamma} - \tfrac{1}{2}\kappa) \pm \{[\bar{\gamma}n - (\gamma_1 - \kappa + \tfrac{1}{2}\bar{\gamma})]^2 + 3\bar{\gamma}^2 n(n-1)\}^{1/2}, \quad (35)$$

$$\epsilon^{\pm}_{\beta}(n) = \gamma_1 n - (\tfrac{1}{2}\gamma_1 - \gamma' + \tfrac{1}{2}\kappa) \pm \{[\gamma' n + (\gamma_1 - \kappa - \tfrac{1}{2}\gamma')]^2 + 3\gamma''^2 n(n-1)\}^{1/2}, \quad (36)$$

where $n = 2, 3, 4, \ldots$, for the minus (−) sign, and $n = 0, 1, 2, \ldots$, for the plus (+) sign in Eqs. (35) and (36). Here the plus sign refers to the spectrum of light-hole energy levels; the minus sign refers to the spectrum of heavy-hole levels. The subscripts α and β can now be identified, respectively, with each member of the pair of original Kramers' doublets.

Energy levels resulting from this calculation will reflect a spherical average over the system. The eigenvalues are given explicitly by Eqs. (35) and (36), and the calculated results are shown in Table II for $H = 100$ kG. Comparison of Tables I and II indicates a fairly close agreement between the individual energy levels from the two calculations. This is to be expected from the nearly spherical energy surfaces at $H = 0$.

The energy levels for both the spherical approximation and the [111] direction are shown in Fig. 2. The nonclassical behavior of the degenerate valence bands is strikingly manifest in the nonuniform spacing of the energy levels for low values

TABLE II. ZnTe energy levels in the spherical approximation $H=100$ kG.

n	ϵ_α^+	ϵ_β^+	ϵ_α^-	ϵ_β^-
0	12.73	23.60	...	...
1	38.69	72.31	...	...
2	79.04	127.78	10.72	6.46
3	131.18	185.61	33.24	23.29
4	187.83	244.39	51.25	39.18
5	246.16	303.63	67.63	54.61
6	305.11	363.12	83.31	69.78
7	364.46	422.77	98.62	84.79
8	424.02	482.52	113.72	99.71
9	483.71	542.34	128.69	114.55
10	543.49	602.21	143.58	129.35
11	603.33	662.11	158.41	144.11
12	663.21	722.04	173.19	158.85
	light holes		heavy holes	

(Energies are in cm^{-1} at $k_H=0$)

of n. The uniform spacing at high quantum numbers is also evident. The level spacings in this regime yield the effective masses given by the classical cyclotron resonance experiment.

C. Case 3: approximate solution in the $(1\bar{1}0)$ plane

For this case, it was possible for Luttinger to use perturbation theory on the difference between the Hamiltonians corresponding to Cases 1 and 2.

The matrix D is separated into three terms,[3]

$$D=D_0+D_1+D_2. \tag{37}$$

As in Case 2, D_0 can be put in 2×2 block form with the solutions

$$\epsilon_\alpha^{\pm}(n)=\gamma_1 n-(\tfrac{1}{2}\gamma_1+\gamma'-\tfrac{1}{2}\kappa) \pm\{[\gamma' n-(\tfrac{1}{2}\gamma'+\gamma_1-\kappa)]^2+3\gamma''^2 n(n-1)\}^{1/2}, \tag{38}$$

$$\epsilon_\beta^{\pm}(n)=\gamma_1 n-(\tfrac{1}{2}\gamma_1-\bar{\gamma}+\tfrac{1}{2}\kappa) \pm\{[\bar{\gamma} n+(\gamma_1-\kappa-\tfrac{1}{2}\bar{\gamma})]^2+3\bar{\gamma}^2 n(n-1)\}^{1/2}. \tag{39}$$

As in Case 2, $n=0,1,2,\ldots$, for the plus sign, and $n=1,2,3,\ldots$, for the minus sign. The new constants γ' and γ'' are expressed by (in a form given by Roth *et al.*[9]),

$$\gamma'=\gamma_3+(\gamma_2-\gamma_3)[\tfrac{1}{2}(3\cos^2\theta-1)]^2, \tag{40}$$

$$\gamma''=\tfrac{2}{3}\gamma_3+\tfrac{1}{3}\gamma_2+\tfrac{1}{6}(\gamma_2-\gamma_3)[\tfrac{1}{2}(3\cos^2\theta-1)]^2, \tag{41}$$

where θ is the angle between the magnetic field and the [001] crystallographic axis in the $(1\bar{1}0)$ plane.

Most of the anisotropy and all of the isotropic part of D is contained in D_0. The D_1 term in Eq. (37) is proportional to $\frac{1}{4}\sqrt{3}(\gamma_2-\gamma_3)$ and will be neglected here since the actual amount of anisotropy in ZnTe is small. The D_2 term in Eq. (37) is proportional to q and hence will be dropped.

Calculated results for the shallowest light-hole state $\epsilon_\alpha^+(0)$, $\epsilon_\beta^+(0)$ are shown in Fig. 3. The energy levels are plotted as functions of the angle θ between the magnetic-field direction and the [001] axis of the crystal, in the $(1\bar{1}0)$ plane. Results for the first two heavy-hole states are shown in Figs. 4 and 5.

In these figures, the dashed lines indicate the results of the spherical approximation (Table II); the black dots are the results of the "exact" [111] calculation (Table I). As expected, the heavy-hole levels suffer more from the effects of anisotropy than do the light holes. However, an interesting effect is that the α and β light-hole states curve in opposite directions, whereas the α and β heavy-hole states curve in the same direction. The very slight departure of the [111] calculations from the plotted curves is in part due to the neglect of the D_1 term. If need be, anisotropy of higher quantum number levels can be readily computed.

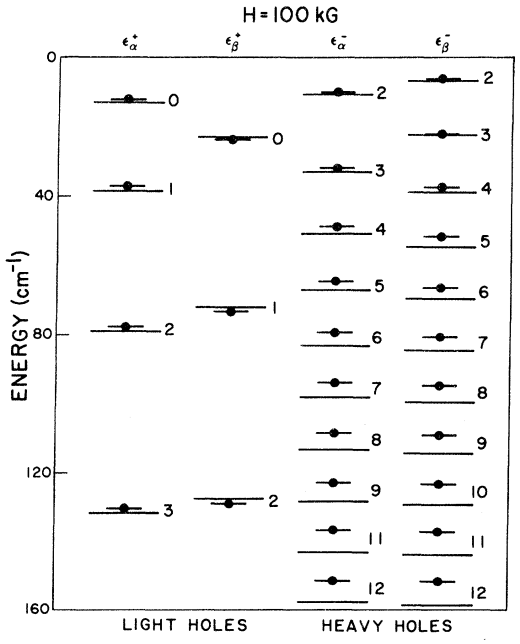

FIG. 2. ZnTe theoretical valence-band energy levels for a field of $H=100$ kG. Long horizontal lines are the results of the spherical approximation. Short lines with dots are from the "exact" calculation in the [111] direction.

IV. MOMENTUM EFFECTS

The results of Luttinger and Kohn apply only to the case of zero momentum along the magnetic-

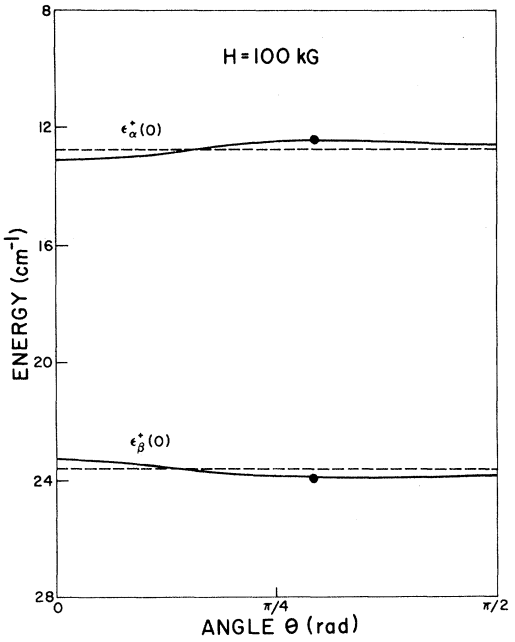

FIG. 3. Anisotropy of the light hole $n=0$ energy levels. Dashed line is the spherical approximation result, and the dot is the "exact" calculation in the [111] direction.

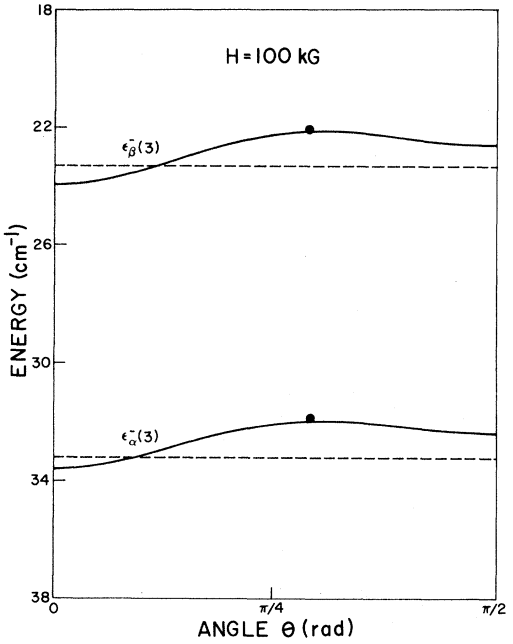

FIG. 5. Anisotropy of the heavy hole $n=3$ energy levels. Dashed line is the spherical approximation result, and the dot is the "exact" calculation in the [111] direction.

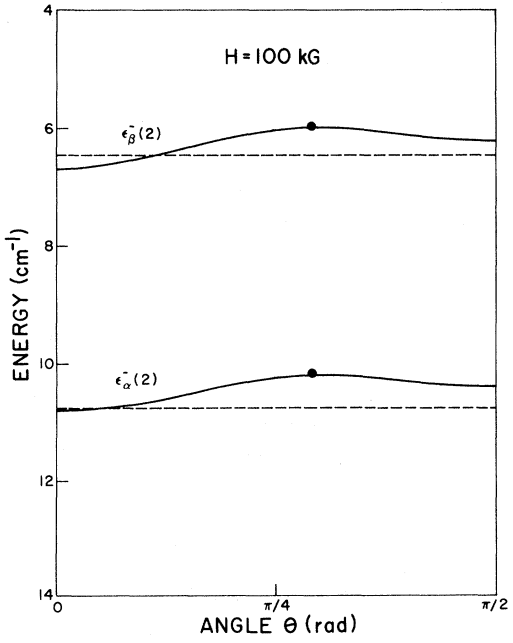

FIG. 4. Anisotropy of the heavy hole $n=2$ energy levels. Dashed line is the spherical approximation result, and the dot is the "exact" calculation in the [111] direction.

field direction. When the population of free holes is low, only $k_H=0$ excitations are possible. However, for large numbers of holes (created thermally or by photoexcitation), k_H-dependent effects may become important. Indeed, Luttinger has pointed out that the valence-band energy levels will depend parametrically on k_H in some involved way.

Goodman[13] has investigated the quantum theory of cyclotron resonance absorption and has discussed line-shape effects as well as new absorption lines which can arise because of $k_H \neq 0$ effects.

Wallis and Bowlden[14] were able to derive the k_H dependence of valence-band energy levels in the presence of a magnetic field, with the restriction that the energy surfaces are spherical. Their results will be summarized here.

The starting point is the Luttinger Hamiltonian, Eq. (10). Wallis and Bowlden chose a specific representation for J such that

$$J_x = \frac{\hbar}{2}\begin{bmatrix} 0 & 0 & \sqrt{3} & 0 \\ 0 & 0 & 2 & \sqrt{3} \\ \sqrt{3} & 2 & 0 & 0 \\ 0 & \sqrt{3} & 0 & 0 \end{bmatrix}, \tag{42}$$

$$J_y = \frac{\hbar}{2}\begin{bmatrix} 0 & 0 & -i\sqrt{3} & 0 \\ 0 & 0 & 2i & -i\sqrt{3} \\ i\sqrt{3} & -2i & 0 & 0 \\ 0 & i\sqrt{3} & 0 & 0 \end{bmatrix}, \tag{43}$$

$$J_z = \frac{\hbar}{2}\begin{bmatrix} 3 & 0 & 0 & 0 \\ 0 & -1 & 0 & 0 \\ 0 & 0 & 1 & 0 \\ 0 & 0 & 0 & -3 \end{bmatrix}. \tag{44}$$

In the spherical approximation, $\gamma_2 = \gamma_3 = \bar{\gamma}$. The parameter q is also taken to be negligibly small. Under these conditions and the ansatz[14]

$$\psi = \begin{bmatrix} c_1 G_n \\ c_2 G_{n+2} \\ c_3 G_{n+1} \\ c_4 G_{n+3} \end{bmatrix}, \tag{45}$$

where the c_n are numerical coefficients, and where[14]

$$G_n = \frac{\exp[i(q_x x + k_H z)]}{(L_x L_z)^{1/2}} \left(\frac{s^{1/2}}{2^n n!\, \pi^{1/2}}\right)^{1/2} H_n(t)\, e^{-t^2/2}, \tag{46}$$

the Schrödinger equation $D\psi = E\psi$ can be solved. In Eq. (46), q_α are momentum eigenvalues, with $q_z \equiv k_H$,

$$t = \sqrt{s}\, y - (q_x/\sqrt{s}), \tag{47}$$

where

$$s = eH/\hbar c, \tag{48}$$

and $H_n(t)$ is the Hermite polynomial of degree n. The functions G are normalized in a box of dimensions L_x, L_y, and L_z and satisfy the operator relations

$$(k_x^2 + k_y^2)\, G_n = \hbar^2 s(2n+1)\, G_n, \tag{49}$$

$$(k_x + ik_y)\, G_n = -\hbar^2\sqrt{s}\,[2(n+1)]^{1/2} G_{n+1}, \tag{50}$$

$$(k_x - ik_y)\, G_n = -\hbar^2\sqrt{s}\,(2n)^{1/2} G_{n-1}, \tag{51}$$

$$k_z G_n = \hbar\sqrt{s}\,\zeta G_n, \tag{52}$$

where

$$\zeta = k_H/\sqrt{s}. \tag{53}$$

The resulting purely numerical matrix D is given by[14]

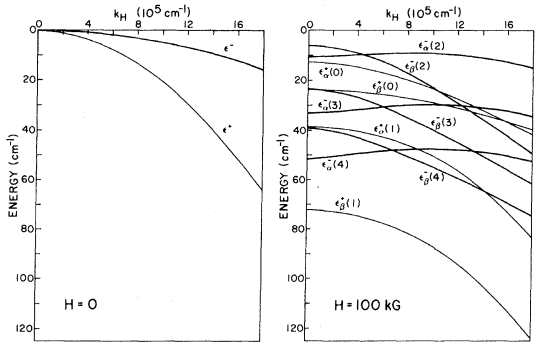

FIG. 6. k_H dependence of the ZnTe energy levels at $H = 0$ and 100 kG. First two light-hole levels and the first three heavy-hole levels are plotted.

$$D = \begin{bmatrix} h_1 & h_2 & h_3 & 0 \\ h_2 & h_4 & 0 & h_5 \\ h_3 & 0 & h_6 & h_7 \\ 0 & h_5 & h_7 & h_8 \end{bmatrix}, \tag{54}$$

where

$$h_1 = (\gamma_1 + \bar{\gamma})(n + \tfrac{1}{2}) + \tfrac{1}{2}(\gamma_1 - 2\bar{\gamma})\zeta^2 + \tfrac{3}{2}\kappa, \tag{55}$$

$$h_2 = -\bar{\gamma}\,[3(n+1)(n+2)]^{1/2}, \tag{56}$$

$$h_3 = \bar{\gamma}\,[6(n+1)]^{1/2}\zeta, \tag{57}$$

$$h_4 = (\gamma_1 - \bar{\gamma})(n + \tfrac{5}{2}) + \tfrac{1}{2}(\gamma_1 + 2\bar{\gamma})\zeta^2 - \tfrac{1}{2}\kappa, \tag{58}$$

$$h_5 = -\bar{\gamma}\,[6(n+3)]^{1/2}\zeta, \tag{59}$$

$$h_6 = (\gamma_1 - \bar{\gamma})(n + \tfrac{3}{2}) + \tfrac{1}{2}(\gamma_1 + 2\bar{\gamma})\zeta^2 + \tfrac{1}{2}\kappa, \tag{60}$$

$$h_7 = -\bar{\gamma}\,[3(n+2)(n+3)]^{1/2}, \tag{61}$$

$$h_8 = (\gamma_1 + \bar{\gamma})(n + \tfrac{7}{2}) + \tfrac{1}{2}(\gamma_1 - 2\bar{\gamma})\zeta^2 - \tfrac{3}{2}\kappa. \tag{62}$$

The energy levels can be determined numerically by solving the secular equation corresponding to Eq. (54). If the parameter ζ is set equal to zero in Eqs. (55)–(62), corresponding to $k_H = 0$, the eigenvalues of Eq. (54) reduce to those of the spherical approximation (Case 2), Eqs. (35) and (36).

Equations (54)–(62) were used to compute the matrix D, and the secular equation was solved for various values of magnetic field and wave vector k_H. Results are presented in Fig. 6, for $H = 0$ and 100 kG. At $H = 0$, the solution reduces to degenerate sets of ϵ^- heavy holes and ϵ^+ light holes. As the magnetic field increases, the levels move to higher energies and separate into orbital ladders and spin levels as shown. The first three ϵ^- levels and the first two ϵ^+ levels are plotted in Fig. 6. The energies at $k_H = 0$ are those given in Table II. A strange feature of the heavy-hole

levels is that at $k_H = 0$ the β-spin state lies higher than the α-spin state, but these two states cross over and order like light-hole states at large values of k_H. Also, the ϵ_α^- states exhibit a negative mass character in the region near $k_H = 0$. This general behavior has been discussed by Wallis and Bowlden.[14]

The light-hole levels are much less perturbed. However, the levels $\epsilon_\alpha^+(0)$ and $\epsilon_\beta^+(0)$ initially follow a curvature characteristic of light holes, but then at large k_H, they assume the curvature of the heavy-hole band, with the α and β states switching in the process. All other light-hole levels follow nearly parabolic curvatures. It should be noted that whereas all levels vary linearly with field at $k_H = 0$, they depart from linear dependence on field at finite values of k_H.

V. RESULTS AND CONCLUSIONS

Theoretical values of the energy levels were computed in Secs. III and IV for a field of 100 kG. Not all of these levels will be populated with holes. In fact, only the shallowest levels are expected to be of interest in a light-scattering experiment. These levels can be populated thermally and by photoexcitation from the laser light.

Although many different transitions between the levels are allowed, we are concerned here with transitions which change the spin quantum number by unity, and leave the principle quantum number n unchanged. The g value is given by

$$g = (2\pi c\hbar/\mu_B)(\omega/H), \tag{63}$$

$$= 2.1428\times10^4(\omega/H), \tag{64}$$

where ω is given in cm^{-1}, and H is given in Gauss. In Eqs. (63)–(64),

$$\omega = |\epsilon_\alpha - \epsilon_\beta|. \tag{65}$$

From Tables I and II, the shallowest light-hole level yields

$$g_{lh}^{[111]}(0) = 2.47 \tag{66}$$

for the [111] direction, and

$$g_{lh}^{av}(0) = 2.33 \tag{67}$$

for the spherical approximation.

For the first two heavy-hole levels,

$$g_{hh}^{[111]}(2) = 0.893, \tag{68}$$

and

$$g_{hh}^{[111]}(3) = 2.11 \tag{69}$$

for the [111] direction, and

$$g_{hh}^{av}(2) = 0.915, \tag{70}$$

and

$$g_{hh}^{av}(3) = 2.14 \tag{71}$$

for the spherical approximation. [Note that the shallowest light-hole (lh) level is denoted by (0), whereas the shallowest heavy-hole (hh) is denoted by (2).]

Anisotropy of the g values in the $(1\bar{1}0)$ plane can be determined from Figs. 3–5. The results are shown in Fig. 7. Heavy-hole g values are only slightly affected by the anisotropy, whereas the light-hole g value varies considerably with the angle θ.

All of the above results are valid for spin-flip transitions between hole levels with hole momentum $k_H \approx 0$. For finite values of k_H, the more complicated behavior implied by Fig. 6 is expected.[1]

Of course, the theoretical calculations of this paper are only as good as the input data, i.e., the cyclotron resonance parameters of Stradling.[12] In an effort to determine how sensitive the theoretical calculations are to variation of these input parameters, each of the parameters was independently varied in a symmetrical fashion about its $\pm\sigma$ error limits. The appropriate Gaussian weighting factor was then assigned to each parameter and the g value was computed. A total of 125 calculations were made, with five different values for each parameter. Each calculation was then weighted by the product of the Gaussian weights for each input parameter. The results are shown in histogram form in Fig. 8. The abscissa represents the g value and the ordinate is the accumulated statisti-

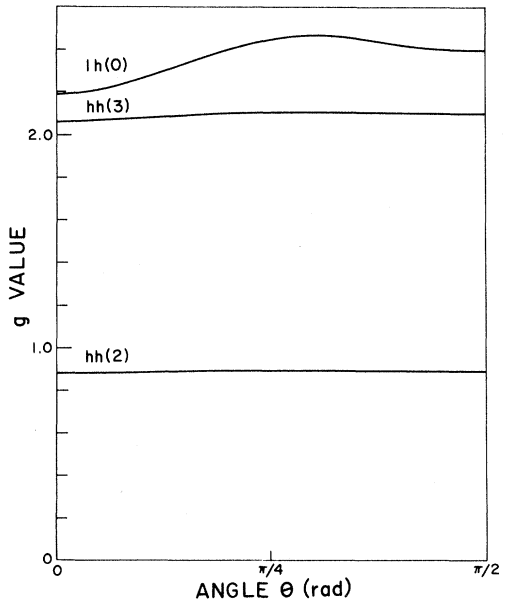

FIG. 7. Anisotropy of the ZnTe light- and heavy-hole g values.

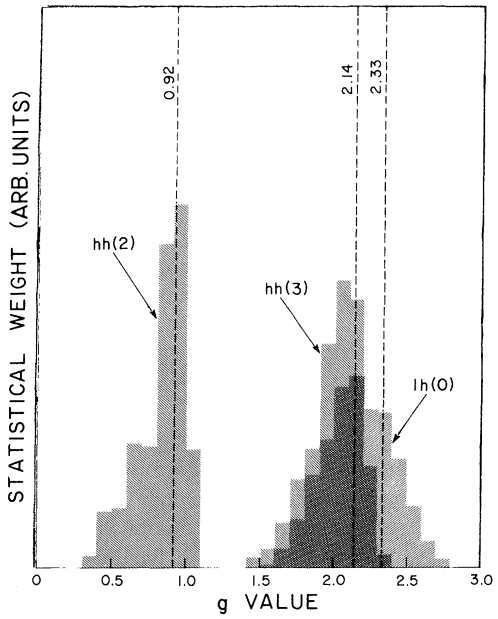

FIG. 8. Statistical results for the theoretical g-value calculations for the first light-hole spin-flip transition and the first two heavy-hole transitions. Dashed lines are the result of the spherical approximation for nominal values of the cyclotron resonance parameters.

cal weight. The calculations were all done in the spherical approximation.

These results show that the most probable heavy-hole ($n=2$) g value lies between $g=0.9$ and $g=1.0$, with the likelihood of other g values being much less. Similar results are shown for heavy holes ($n=3$) and for light holes ($n=0$). The g values for nominal input parameters [see Eqs. (16)–(18)] are indicated by dashed lines. The widths of these histograms yield a rough measure of how errors in the input to the theory are mapped into the final results. In this way, the *theoretical* error limits can be applied (for the spherical approximation case):

$$g_{\mathrm{hh}}^{\mathrm{av}}(2)=0.92\pm0.15, \tag{72}$$

$$g_{\mathrm{hh}}^{\mathrm{av}}(3)=2.14\pm0.20, \tag{73}$$

$$g_{\mathrm{lh}}^{\mathrm{av}}(0)=2.33\pm0.40. \tag{74}$$

Similar error limits hold for calculations in the [111] direction and in the $(\bar{1}10)$ plane.

The 4×4 formalism of Luttinger and Kohn applies to the fourfold-degenerate valence band, and is strictly correct only when there are no nearby perturbing bands. This is not the case, however, for many narrow-gap semiconductors, but it is satisfied to a good degree in ZnTe, where the conduction band lies at $E_g=2.391$ eV,[15] and the split-off band lies at $\Delta=0.93$ eV,[16] away from the degenerate valence band.

For their theoretical calculations on Ge, Roth *et al.*[9] employed a 6×6 formalism, taking into account the split-off band. They concluded that for Ge, the effect of the split-off band on the heavy-hole levels could be neglected. The question then arises: Why don't valence-band energy levels of the 4×4 formalism depend on the magnitude of the spin-orbit parameter? Evidently the spin-orbit parameter enters only for large values of k_H. According to Yafet,[10] the energy levels are independent of Δ as long as the kinetic energy is small compared to Δ. The energy levels are determined by the band shape, i.e., the parameters A, B, and C as obtained in the classical cyclotron resonance experiment, in conjunction with the additional parameter κ.

For InSb, Pidgeon and Brown[17] have gone to an 8×8 formalism based on the Luttinger-Kohn theory, where in addition to the split-off band, the conduction band is also included. This is necessary for InSb, because of its small band gap. For this treatment, it is necessary to know the value of the interband momentum matrix element P^2 defined by Kane.[18] For ZnTe, the parameter P^2 is unknown, but estimates[19] for II-VI compounds yield $P^2\sim21$ eV. The principle effect of the more-complicated 8×8 formalism is a small sublinear dependence of the energy levels on the magnetic field. For ZnTe, this should be negligible.

Finally, it should be mentioned that a generalization of the 8×8 formalism to include an infinite series of harmonic oscillator functions was developed by Bell and Rogers[20] for InSb. As with the 8×8 treatment, this further complexity is not warranted for the case of ZnTe.

*Work supported by NSF Grant No. GH-34681, by the U. S. Air Force, contract F 33615-74-C-4018 (Aerospace Research Laboratories, Wright-Patterson AFB), and by AFOSR Grant No. 75-2835.

†Present address: NSF-CNRS Exchange Scientist, Université Pierre et Marie Curie, Paris, France.

[1]R. L. Hollis and J. F. Scott, following paper, Phys. Rev. B 15, 942 (1977).

[2]J. M. Luttinger and W. Kohn, Phys. Rev. 97, 869 (1955).

[3]J. M. Luttinger, Phys. Rev. 102, 1030 (1956).

[4]Y. Yafet, Phys. Rev. 152, 858 (1966).

[5]See, for example, C. Kittel, *Quantum Theory of Solids* (Wiley, New York, 1963), p. 268.

[6]See, for example, L. I. Schiff, *Quantum Mechanics* (McGraw-Hill, New York, 1968), p. 227.

[7]H. J. Zeiger and G. W. Pratt, *Magnetic Interactions in Solids* (Oxford U. P., London, 1973), p. 397.
[8]G. Dresselhaus, A. F. Kip, and C. Kittel, Phys. Rev. 98, 368 (1955).
[9]L. M. Roth, B. Lax, and S. Zwerdling, Phys. Rev. 114, 90 (1959).
[10]Y. Yafet, in *Solid State Physics*, edited by F. Seitz and D. Turnbull (Academic, New York, 1963), Vol. 14, p. 31.
[11]W. Kohn (unpublished results).
[12]R. A. Stradling, Solid State Commun. 6, 665 (1968).
[13]R. R. Goodman, Ph.D. thesis (University of Michigan, 1958) (unpublished).
[14]R. F. Wallis and H. J. Bowlden, Phys. Rev. 118, 456 (1960).
[15]A. C. Aten, C. F. Van Doorn, and A. T. Vink, in *Proceedings of the International Conference on the Physics of Semiconductors, Exeter, 1962*, edited by A. C. Strickland (The Institute of Physics and the Physical Society, London, 1962), p. 696.
[16]M. Cardona, K. L. Shaklee, and F. H. Pollak, Phys. Rev. 154, 696 (1967).
[17]C. R. Pidgeon and R. N. Brown, Phys. Rev. 146, 575 (1966).
[18]E. O. Kane, J. Phys. Chem. Solids 1, 249 (1957).
[19]M. Cardona, J. Phys. Chem. Solids 24, 1543 (1963).
[20]R. L. Bell and K. T. Rogers, Phys. Rev. 152, 746 (1966).